

Non-Contact Determination of Vital Signs Monitoring of Animals in Hemorrhage States Using Bio-Radar

Xiao Yu¹, Yue Yin^{1, 2}, Hao Lv¹, Yang Zhang¹,
Fulai Liang¹, Pengfei Wang¹, and Jianqi Wang^{1, *}

Abstract—With the rapid development and in-depth research of non-contact bio-radar-based detection technology, researchers have recently been putting more emphasis on target identification. Living status identification, a hotspot of target identification research, is particularly useful in search and rescue missions. During such missions, in order to rescue victims and provide corresponding medical support in a timely manner, it is necessary to acquire the survival information of victims, especially when they are injured. Hence, the vital signs extracted from a radar signal should be considered as the crucial parameters to reflect the living status. To determine living status through analyzing vital signs, this study utilized a bio-radar system to continuously monitor hemorrhagic animals, which simulated injured persons with hemorrhagic symptoms. Moreover, we defined and classified three survival periods based on changes in vital signs combined with a K-nearest neighbor algorithm (KNN) classifier. Experimental results show that we can approximately determine the current living status of animals with this method, which can aid in providing information for on-site rescue and follow-up medical treatment.

1. INTRODUCTION

Previous studies have confirmed that radar is an effective instrument in non-contact detection, which shows great potential in multiple applications, such as disaster rescue, terrorist activity identification, and medical monitoring [1–7]. It is well established that in disasters such as earthquakes, landslides, and terrorist attacks, the most pressing goal is to rescue victims. Until now, studies on bio-radar have basically accomplished human presence detection behind barriers. At present, most research is focusing on the location, number, and movement of targets [8–12]. With the further development of bio-radar technology, an increasing number of studies are putting more emphasis on target identification to acquire valuable information through bio-radar, which we think will become a hotspot in non-contact life detection research [13–16].

Target identification mainly includes three aspects: human and animal distinction, living status identification, and accurate individual identification. Our team has reported the use of bio-radar to locate and detect the respiration and heartbeats of healthy persons behind obstacles [17–22]. However, under a complex rubble environment, there exists the possibility that some animals are also present, and since the vital signs of humans and animals are similar, misjudgment may occur. To solve this problem, we have proposed some novel methods to distinguish between humans and animals [23–25]. During search and rescue missions, the survival condition of a victim is an essential piece of information for the diagnosis and treatment of injury. After distinguishing the correct human body buried under rubble, the next task is to acquire their current physiological status. It is best if we can extract the survival information from the received radar signal to determine the living status of victims. The survival information can aid in decision-making about the priority for rescuing injured persons and allocating

Received 27 October 2020, Accepted 21 December 2020, Scheduled 25 December 2020

* Corresponding author: Jianqi Wang (wangjq@fmmu.edu.cn).

¹ Department of Biomedical Engineering, Fourth Military Medical University, Xi'an, China. ² Department of Medical Engineering, The General Hospital of Western Theater Command PLA, Chengdu, China.

medical resources more reasonably. Besides, with the help of valuable survival information, the working efficiency can be largely enhanced, and victims can be rescued and cured in time.

Hemorrhage is the leading cause of morbidity and mortality in surgery and trauma patients [26]. During natural disasters or anti-terrorist missions, individuals often suffer traumatic injuries, and blood loss is one of the most common symptoms. Rescuers should monitor the current vital signs of injured persons derived from radar to reflect their life status. Given this factor, some groups have studied the detection and monitoring of injured subjects. A research group in Japan reported that they could distinguish a hypovolaemic group of rabbits from a normal group using radar, but the living statuses in the two groups were changeless [27]. The Chinese Academy of Sciences continuously monitored the vital signs of Beagle dogs and Wistar rats with different injuries and summarized four survival periods according to variational life signals [28]. However, since the sensors used in this study were contact type and wearable, they were a source of outside disturbance to the animals. Furthermore, the above studies mainly focused on the rate variables of heartbeats and respiration, which may not totally determine the condition of subjects, since the single rate feature cannot completely describe signal characteristics in complicated situations.

Due to the time-varying, non-stationary, and nonlinear characteristics of biomedical signals, time-frequency analysis is a suitable choice for analyzing these signals and providing the instantaneous frequency and amplitude. Additionally, the non-contact detection mode of radar is suitable for animal experiments, since it does not constrain the animals or cause any obvious outside effects. Based on the advantages of radar detection and time-frequency analysis, this study explores the feasibility of using radar to continuously monitor the physiological state of humans suffering from massive hemorrhage and analyzing life signals in the time-frequency field. The goal was to determine the current living status through vital signs derived from radar echo signals.

An experimental hemorrhagic state was produced by arterial blood withdrawal in rabbits. We utilized a physiological signal collection system and a radar system to monitor the vital signs of rabbits simultaneously. Data collected from the physiological signal collection system were considered as the reference information during the experiment. The study defined three periods of the physiological state of an injured rabbit based on the blood pressure variation. To determine the physiological state of animals from the radar echo signal, K-nearest neighbor (KNN) classification was conducted using variables derived from the proposed non-contact method. This technique can be applied to aid in search, rescue, and therapy for deeply buried, injured humans and may aid in vital sign estimation.

The rest of study is organized as follows: Section 2 introduces materials and methods, including monitoring systems, animal experiments, and signal processing methods. The experimental results are described in Section 3. Section 4 gives the discussion on the experimental results. Section 5 ends the paper with a conclusion on existing problems and a description of further research directions.

2. MATERIALS AND METHODS

The goal of this experiment is to monitor changes in the vital signs of rabbits in a hemorrhagic state using bio-radar as well as a contact-type monitoring system. We aim to obtain living status information derived from vital sign changes.

2.1. Contact-type Monitoring System

The RM6240E physiological signal collection system was utilized to acquire blood pressure, respiration, and heartbeat signals, as shown in Figure 1. It has four independent data channels, and the sampling rate can reach up to 100 kHz.

Studies show that mean arterial pressure (MAP) is an important hemodynamic variable which can indicate physiological periods and is associated with increasing hemorrhage volume and mortality [29–31]. In an attempt to better define and characterize the life status of subjects, the MAP parameter was used in this paper for physiological period classification in the contact-type measurements.

According to the measurement of blood pressure of rabbits during the experiment, we defined three survival periods based on MAP variation: normal period (narcosis period), hemorrhage period, and agonal period. Besides, the hemorrhage period can be refined into early hemorrhage compensation

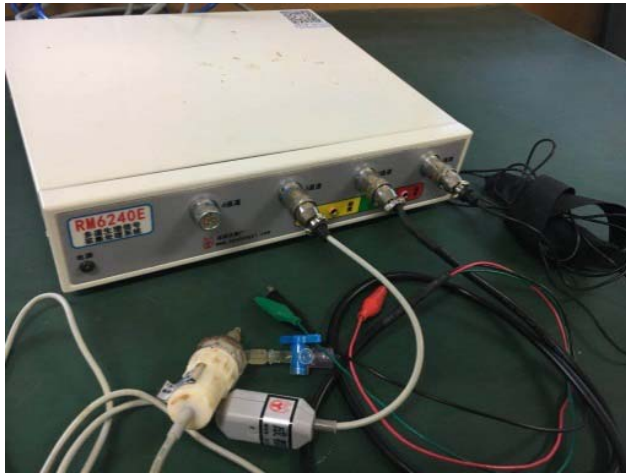


Figure 1. RM6240E physiological signal collection system.

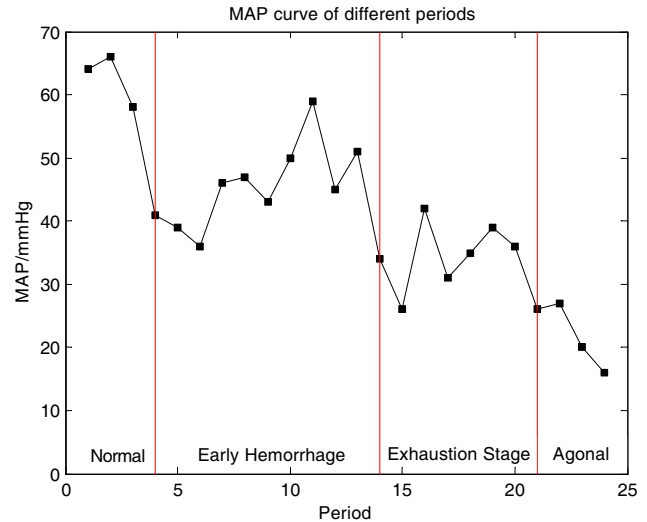


Figure 2. Curve of MAP in different periods.

stage and exhaustion stage. We adopted the fixed-volume hemorrhage method to build the hemorrhagic model, which was accomplished via the withdrawal of blood from the carotid artery. In the normal period, the animals were anesthetized. The vital signs of the rabbits were in the standard scope and were quite stationary under the anesthesia condition. The value of MAP was above 60 mmHg. In the hemorrhage period, as a result of body compensatory mechanisms, animals become restless. Due to blood loss, the ventricular diastolic filling becomes insufficient, and the heart is unable to provide optimal blood flow to cells and tissues. Initially, the arteries constrict and the heartbeat quickens in order to maintain blood pressure and redistribute cardiac output [31]. In the meantime, the amplitude and frequency of breathing increase, and the MAP ranges from 60 mmHg to 40 mmHg. However, the compensatory mechanisms are limited. With the volume of blood loss increasing, the compensatory mechanisms will gradually become invalid, and severe cellular hypoxia and organ damage may occur, which may lead to an exhaustion stage [32]. In the exhaustion stage, the amplitude and frequency of breathing slow down and arrhythmia appears. Furthermore, the MAP fluctuates around 40 mmHg and even below 40 mmHg. When the compensatory mechanisms become totally invalid, the micro-vibration signal gets weak little by little and the subject will reach the agonal period with MAP decreasing continuously, mostly below 30 mmHg. Figure 2 shows the curve of MAP in different survival periods. The MAP variations in all rabbits showed similar trends during observation.

2.2. Non-Contact Monitoring System

The microwave radar technology introduced in this study was developed by our research group. The continuous wave (CW) radar generates a stable microwave at 24 GHz. It is a transmitting and receiving sensor which consists of a transmitting antenna and a receiving antenna. The block diagram of the CW radar system is shown in Figure 3. The radar raw signals are captured by a data acquisition card and processed and displayed on the computer. Figure 4 shows the processing flow of the radar echo signal. After preprocessing, including background removing, low-pass filtering, and adaptive filtering, most noise is eliminated, and effective life signals remain. Then, Fast Fourier Transform (FFT) of the microwave radar analogue output is conducted using an analyzing recorder so as to extract the respiratory signal.

2.3. Signal Entropy

Due to complicated interferences, the life signal transmitted from the radar receiver has a low signal-to-noise ratio (SNR), strong randomness, and low frequency range. Thus, the signal output is nonlinear

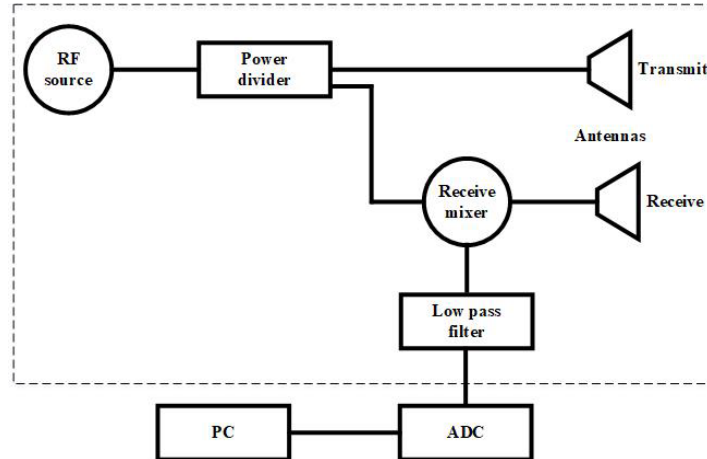


Figure 3. Block diagram of the CW radar system.

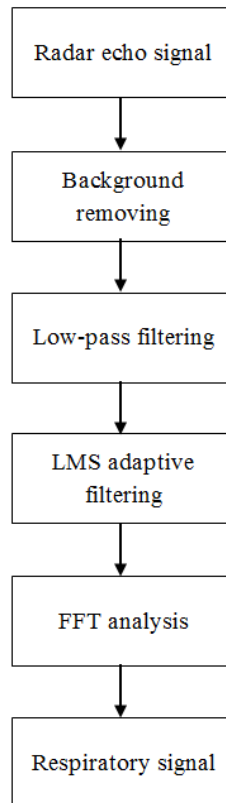


Figure 4. Processing flow of radar echo signal.

and non-stationary. Therefore, a signal processing technique applicable to time-varying signal detection has been demonstrated that permits us to classify physiological periods.

Shannon put forward the concept of “information entropy,” which resolved the problem of quantitative measurement of information and found a unified scientific measurement method for the amount of measurement information [33]. On the basis of the concept of thermodynamic entropy, Shannon referred to the information-excluded redundant average information quantity as “information entropy” and raised the mathematical calculation for information entropy, shown in Function 1 and Function 2. Entropy reflects the average degree of complexity of the information source that can be

defined as a measure of the uncertainty of the quantitative information in a system [34]. A more disordered signal indicates higher entropy.

$$\sum_{i=1}^n p_i = 1. \tag{1}$$

$$H(X) = -\sum_{i=1}^n p(x_i) \log p(x_i). \tag{2}$$

In the above formulas, the information X contains n random events. $p(x_i)$ is the probability of each random event x_i , and $H(X)$ is the entropy of the information X .

According to the non-stationary feature of body vibration signals, entropy information can be applied to this kind of signal analysis. Figure 5 displays the respiratory signal from radar. When animals are in the normal period, the micro-vibration signal of radar is stationary, and the entropy value is calculated as 1.56. In the hemorrhage period, the micro-vibration signal is non-stationary and time-varying because of compensatory mechanisms. If the blood loss volume is too heavy to compensate, the animal will tend to experience body failure. During this period, the signal becomes complex and disordered, and the entropy value is correspondingly higher: 3.31. In the agonal period, the micro-vibration signal becomes more disordered and finally disappears. The entropy value is still at a high degree: 3.08, but there appears to be a decreasing trend of amplitudes corresponding to a decreasing breathing frequency. From the above description, the entropy fluctuates from low to high in different periods. Although the entropies between the normal and agonal periods are somewhat similar, the amplitude of the agonal period is obviously the minimum among all three periods. The results presented here demonstrate that the entropy combined with the amplitude parameter can basically identify three survival periods of targets. In order to obtain more accurate classification of survival periods, we also add the frequency feature in classification.

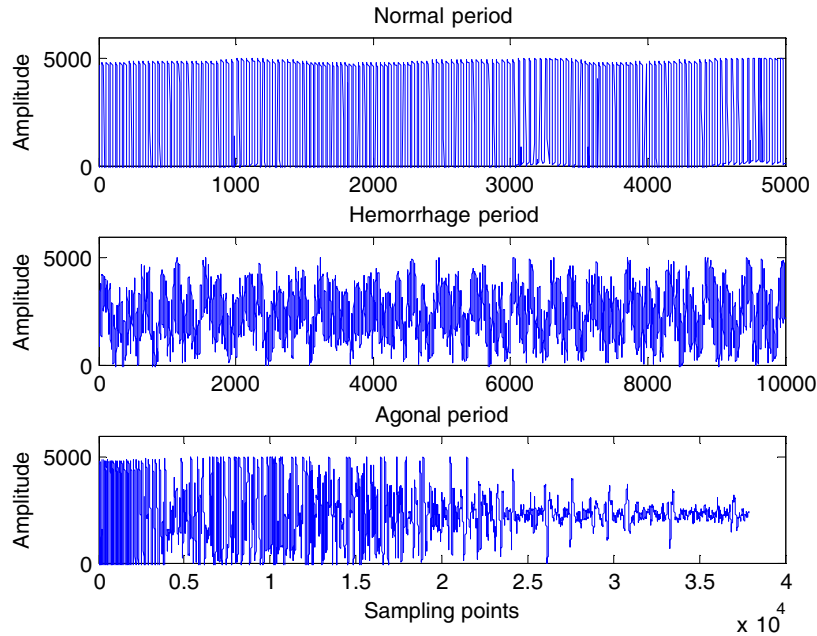


Figure 5. Respiratory signal of three survival periods from radar.

2.4. K-nearest Neighbors Classifier

The K-nearest neighbor algorithm (KNN) is a common classification algorithm in machine learning, which was first proposed by Cover and Hart [35]. KNN has become a very effective non-parametric

classification algorithm, which is widely used in multiple applications such as pattern recognition, statistical classification, computer vision, and DNA sequencing [36].

KNN is a lazy learning process that simply stores known training data. The core concept is that if the majority of nearest neighbors of a sample belong to a certain category, the sample also belongs to this category and possesses characteristics of this category. The classification method is based on selecting the k -th neighbors with minimum eigenvector distances between the known training dataset and the test dataset. In k -th minimum distances, the major category of these k -th neighbors determines the final category of the testing sample. The classifying steps are described as follows:

Step 1: Calculate distances between the testing data and each set of training data. The Euclidean distance was used in this study, shown in Function 3.

$$d(x, y) = \sqrt{\sum_{i=1}^n (x_i - y_i)^2}, \quad (3)$$

where $X = (x_1, x_2, \dots, x_n)$ and $Y = (y_1, y_2, \dots, y_n)$ represent the data of two samples, and n is the number of eigenvectors.

Step 2: Sort distances by ascending order.

Step 3: Select k -th minimum distances.

Step 4: Calculate frequencies of categories of k -th neighbors.

Step 5: Determine the category of the testing data. The majority voting in the neighborhood is the predicted category of the testing data.

KNN has many advantages, such as simple concept, high accuracy, and low sensitivity to abnormal values, and it can be used either in classification or regression. This paper chose KNN to classify survival periods because of its good generalization, easy implementation, and better accuracy in multi-classification [37]. Besides, KNN appears particularly suitable to classify intersectional or overlapped testing data because it classifies based on nearby samples rather than directly determining the class label. The data in this experiment have some overlaps, which is another reason why we choose KNN.

3. RESULTS

3.1. Animal Experiments

Nine New Zealand rabbits, each weighing approximately 2.5 kg, were anesthetized by intraperitoneal injection of 25% urethane at 5 ml per kilogram of body weight. After anesthetization, rabbits were fixed on the operating table in the supine position and remained fully anesthetized throughout the experiment. The monitoring time was 30 min under the anesthetic condition. Then, the right carotid artery of each rabbit was isolated and cannulated using an arterial catheter. A t-branch pipe was connected to the arterial catheter in order to control blood withdrawal and monitor blood pressure. The hemorrhage period was induced by withdrawal of 4 ml/kg blood each time from the carotid artery catheter with a monitoring interval of 30 minutes. Moreover, the speed of withdrawal was about 2 ml/(kg*min). When the subject reached the agonal period, we stopped blood drawing and monitored until death. The radar was placed 30 cm away from the side abdomen of the rabbit to monitor the respiratory signal. The experiment setup is shown in Figure 6.

To compare the results of the proposed non-contact method with those of the contact method, the abdominal position with the most obvious respiratory fluctuation of rabbits was fixed with the tie-on respiratory transducer to measure the respiratory signal. The output breathing signal was the first data channel of the RM6240E physiological signal collection system. The electrocardiogram was recorded as the second data channel by subcutaneous insertion using the limb lead. To monitor the blood pressure associated with the physiological periods, a pressure transducer was connected to one side of the t-branch pipe. The carotid arterial pressure signal output was the third data channel.

All experiments were conducted in accordance with the guidelines of AirForce Military Medical University Medical Ethics Committee and were in compliance with the Declaration of Helsinki.

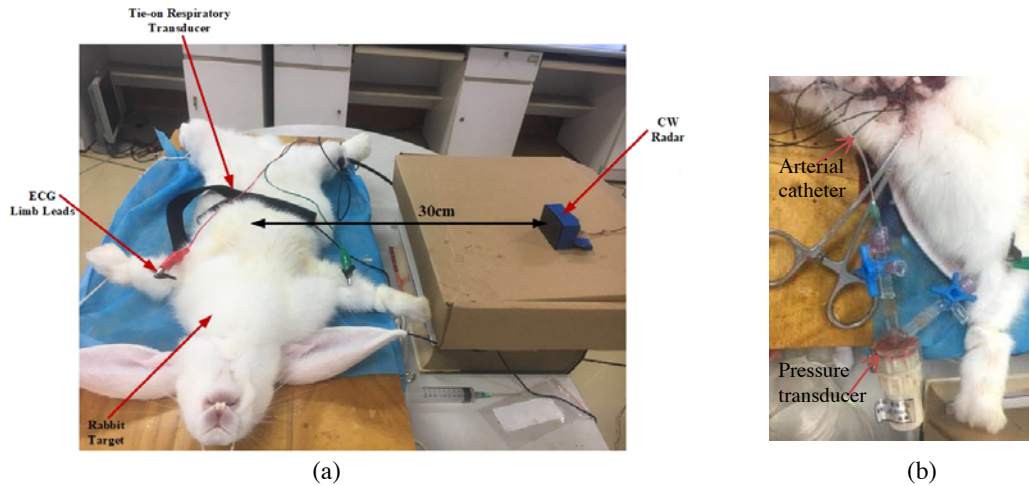


Figure 6. (a) The monitoring experiment setup. (b) The hemorrhage experiment setup.

3.2. Experimental Results

The respiratory rates were determined by the proposed non-contact method correlated significantly with the respiratory rates measured by the respiration transducer, as shown in Figure 7. The fitting curve was

$$y = 1.008 * x + 0.8049 \tag{4}$$

where x is the contact respiration rate, and y is the non-contact respiration rate. The correlation coefficient was $R^2 = 0.9979$, indicating that the radar respiration measurement was accurate.

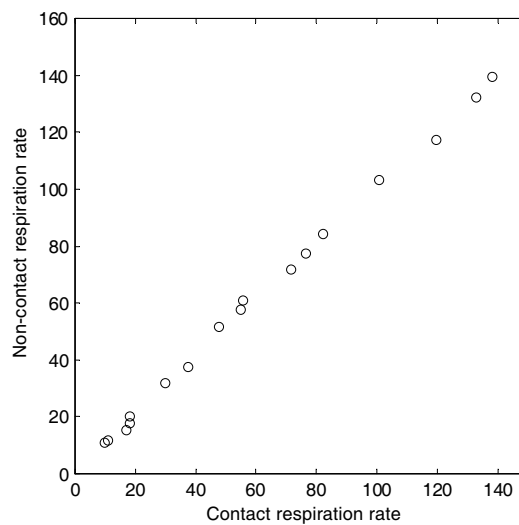


Figure 7. Respiratory rates measured by contact and non-contact methods.

The radar data collected were divided into several subsections, and each subsection contained 2400 sampling points (the sampling rate was 40 Hz). The divided subsections data were used in later classification.

In KNN classification, three classes were measured: normal period, hemorrhage period, and agonal period. The radar data of six rabbits were used for the training set (normal: 150 groups, hemorrhage: 500 groups, agonal: 90 groups), and the radar data of the other three rabbits were used for the testing set (normal: 83 groups, hemorrhage: 370 groups, agonal: 42 groups). Since the absolute value of

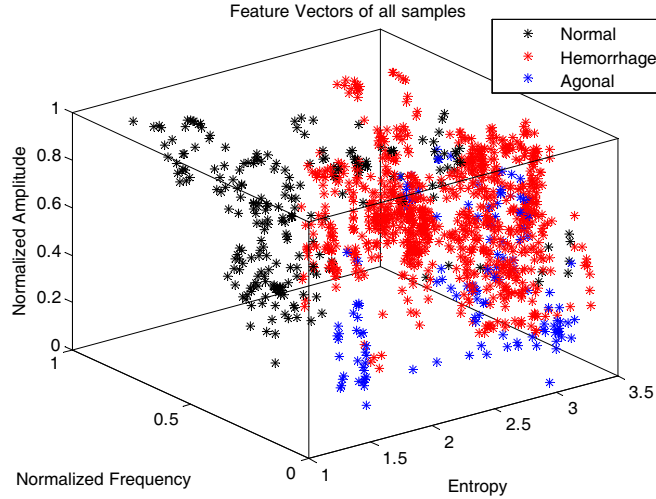


Figure 8. Three-dimensional diagram of feature vectors of all samples.

the amplitude parameter was large, directly substituting the calculation would have resulted in the proportion of the component being too large, so the parameters needed to be normalized. Therefore, the feature vectors were normalized frequency, normalized amplitude, and entropy value of body vibration signal. Figure 8 shows the three-dimensional diagram of feature vectors of all samples.

Because this is a multi-class classification question, we presented three methods to conduct KNN classification and made a comparison among these three methods to find the most suitable method.

Method 1: We conducted three-class classification directly. The predicted results are shown in Table 1 with the classification accuracy of 83.8%. Results show that the normal period is easy to identify. However, hemorrhage and agonal periods have some overlaps. The reason partially lies in the relationship between hemorrhage and agonal periods, as the agonal period is a transition from the hemorrhage period. Thus, these two periods are somewhat similar in terms of vital signs. Given this condition, we set $k = 3$ in the classification, which has better accuracy than one neighbor.

Table 1. Classification results of KNN ($K = 3$).

	Normal (test)	Hemorrhage	Agonal
Normal (predict)	74	30	1
Hemorrhage	9	329	29
Agonal	0	11	12

Method 2: Because both normal and hemorrhagic periods can be considered as the live condition, we unified normal and hemorrhage periods as one live condition and conducted two-class classification between the live condition and agonal period first. The accuracy of the first classification was 87.9%. Then we used two-class classification again between the normal and hemorrhagic periods. Therefore, this method employed two-class classification twice. The accuracy of the second classification was 93.6%. The predicted results are shown in Tables 2 and 3. The total accuracy was 82.3%, which is the result of 87.9% multiplied by 93.6%.

From Table 2, we can see that only 12 sets of agonal data were correctly predicted as the agonal condition. Most of agonal data were classified as the live condition. The reason for the high error rate may be that some agonal periods are transitional periods from the live condition to death. Hence, these agonal periods and some live conditions have similar characteristics. In Table 3, it becomes easy to identify normal and hemorrhage periods, and the accuracy gets higher correspondingly.

Method 3: Similarly, once the hemorrhagic experiment started, both hemorrhagic and agonal

Table 2. The first two-class classification results of KNN ($K = 3$).

	Live (test)	Agonal
Live (predict)	423	30
Agonal	30	12

Table 3. The second two-class classification results of KNN ($K = 3$).

	Normal (test)	Hemorrhage
Normal (predict)	74	20
Hemorrhage	9	350

Table 4. The first two-class classification results of KNN ($K = 3$).

	Normal (test)	Abnormal
Normal (predict)	74	10
Abnormal	9	402

Table 5. The second two-class classification results of KNN ($K = 3$).

	Hemorrhage (test)	Agonal
Hemorrhage (predict)	333	30
Agonal	37	12

periods could be considered as abnormal conditions. The first step was classifying normal and abnormal conditions by two-class classification, and the accuracy was 96.2%. Secondly, the hemorrhagic and agonal periods were classified again, and the accuracy was 83.7%. The predicted results are shown in Tables 4 and 5. The total accuracy was 80.5%.

Abnormal periods are easy to identify in Table 4, as normal periods are the most independent condition in vital signs that can be separated easily from abnormal periods. Due to the same transitional feature, most agonal periods are difficult to identify in Table 5.

4. DISCUSSION

In order to obtain higher classification accuracy, we utilized three methods to classify three periods. Method 1 was a direct three-class classification, and method 2 and method 3 were twice two-class classifications. The total accuracy of each method was 83.8%, 82.3%, and 80.5%, respectively. From the above results, although method 1 had the highest accuracy among the three methods, it did not have satisfactory performance. We think the reason lies in two parts. First, as mentioned before, the data have some overlaps in hemorrhage and agonal periods, and some of the agonal samples are considered as transitional periods. Second, the imbalanced sample size leads to misjudgment. But this factor is unavoidable to a certain extent because the duration of hemorrhage is the longest, and the agonal period lasts only for a short time compared with the other two periods. To solve this problem, we can try other advanced algorithms in dealing with the issue of classification on imbalanced datasets.

5. CONCLUSIONS

In rescue missions, it is of great importance to determine the survival conditions of humans buried under rubble. Radar can be applied as a useful tool to detect the life signals of buried victims. After the detection and location of victims, the next step is to evaluate the survival conditions of subjects in order to provide appropriate medical attention. Thus, extracting survival information from the received life signal is crucial. This study proposed a novel method to extract time-frequency characteristics of body vibration signals from hemorrhagic rabbits and then defined three survival periods using a KNN classifier. In time-frequency analysis, three features of the respiration signal could be acquired: frequency, amplitude, and entropy. Next, three kinds of KNN methods were adopted to classify three survival periods. Results showed that survival periods such as normal period, hemorrhage period, and agonal period could be classified approximately, and the classification accuracies of the three KNN methods were 83.8%, 82.3%, and 80.5%. Based on this idea, we are able to determine the living condition of humans through a received radar echo signal. In future studies, we plan to conduct more animal hemorrhage experiments and expand to a variety of animals such as dogs and pigs to fully evaluate the effectiveness of this method.

ACKNOWLEDGMENT

This work was supported by the National Natural Science Foundation of China (No. 81601567, 61327805) and the Key Research and Development Program of Shaanxi Province (No. 2018SF-170).

AUTHOR CONTRIBUTIONS

Xiao Yu and Yue Yin conceived and designed the experiments and wrote the paper as well. They contributed equally to this work and should be regarded as co-first author. Yue Yin, Yang Zhang and Pengfei Wang performed the experiments; Yue Yin and Hao Lv analyzed the data; Fulai Liang contributed experimental materials. All authors participated in the discussion about the proposal and contributed to the analysis of the results.

REFERENCES

1. Borek, S. E., B. J. Clarke, and P. J. Costianes, "Through-the-wall surveillance for homeland security and law enforcement," *Proc SPIE*, Vol. 5778, 175–185, 2005.
2. Burchett, H., "Advances in through wall radar for search, rescue and security applications," *2006 IET Conference on Crime and Security*, 511–525, London, UK, 2006.
3. Staderini, E. M., "UWB radars in medicine," *IEEE Aeros. Elec. Sys. Mag.*, Vol. 17, No. 1, 13–18, 2002.
4. Ernestina, C. and G. Bharat, "FM-UWB for communications and radar in medical applications," *Wireless. Pers. Commun.*, Vol. 51, 793–809, 2009.
5. Chang, J., C. Paulson, and P. Welsh, "Development of micropower ultrawideband impulse radar medical diagnostic systems for continuous monitoring applications and austere environments," *2012 IEEE Radar Conference*, 699–704, 2012.
6. Gu, C. Z. and C. Z. Li, "From tumor targeting to speech monitoring: Accurate respiratory monitoring using medical continuous-wave radar sensors," *IEEE Microwave Magazine*, Vol. 15, 66–76, 2014.
7. Mostov, K., E. Liptsen, and R. Boutchko, "Medical applications of shortwave FM radar: Remote monitoring of cardiac and respiratory motion," *Medical Physics*, Vol. 37, No. 3, 1332–1338, 2010.
8. Kim, Y., S. Ha, and J. Kwon, "Human detection using doppler radar based on physical characteristics of targets," *IEEE Geoscience and Remote Sensing Letters*, Vol. 12, No. 2, 289–293, 2015.

9. Nanzer, J. A., "A review of microwave wireless techniques for human presence detection and classification," *IEEE Transactions on Microwave Theory and Techniques*, Vol. 65, No. 5, 1780–1794, 2017.
10. Liang, F. L., F. G. Qi, Q. An, H. Lv, F. M. Chen, Z. Li, and J. Q. Wang, "Detection of multiple stationary humans using UWB MIMO radar," *Sensors*, Vol. 16, No. 11, 1922–1938, Basel, Switzerland, 2016.
11. Li, J., Z. Zeng, J. Sun, and F. Liu, "Through-wall detection of human Being's movement by UWB radar," *IEEE Geoscience and Remote Sensing Letters*, Vol. 9, No. 6, 1079–1083, 2012.
12. Thiel, M. and K. Sarabandi, "Ultra wideband multi-static scattering analysis of human movement within buildings for the purpose of stand-off detection and localization," *IEEE Trans. Antennas Propag.*, Vol. 59, 1261–1268, 2011.
13. Van, N., A. Q. Javaid, and M. A. Weitnauer, "Detection of motion and posture change using an IR-UWB radar," *2016 38th Annual International Conference of the IEEE Engineering in Medicine and Biology Society (EMBC)*, 3650–3653, Orlando, FL, USA, 2016.
14. Kiasari, M. A., S. Y. Na, J. Y. Kim, and Y. Won, "Monitoring human behavior patterns using ultra-wide band radar based on neural networks," *Asia Life Sciences*, 13–29, 2015.
15. Zhai, S. J. and T. Jiang, "Target detection and classification by measuring and processing bistatic UWB radar signal," *Measurement*, Vol. 47, 547–557, 2014.
16. Bryan, J. D., J. Kwon, N. Lee, and Y. Kim, "Application of ultra-wide band radar for classification of human activities," *IET Radar, Sonar & Navigation*, Vol. 6, No. 3, 172–179, 2012.
17. Lv, H., G. H. Lu, X. J. Jing, and J. Q. Wang, "A new ultra-wideband radar for detecting survivors buried under earthquake rubbles," *Microwave & Optical Technology Letters*, Vol. 52, No. 11, 2621–2624, 2010.
18. Wang, J. Q., C. X. Zheng, G. H. Lu, and X. J. Jing, "A new method for identifying the life parameters via radar," *EURASIP Journal on Advances in Signal Processing*, Vol. 2007, No. 1, 1–8, 2007.
19. Zhang, Y., F. M. Chen, H. J. Xue, Z. Li, Q. An, J. Q. Wang, and Y. Zhang, "Detection and identification of multiple stationary human targets via bio-radar based on the cross-correlation method," *Sensors*, Vol. 16, No. 11, 1793–1804, 2016.
20. Liang, F. L., F. G. Qi, Q. An, H. Lv, F. M. Chen, Z. Li, and J. Q. Wang, "Detection of multiple stationary humans using UWB MIMO radar," *Sensors*, Vol. 16, No. 11, 1922–1938, Basel, Switzerland, 2016.
21. Lv, H., F. G. Qi, Y. Zhang, T. Jiao, F. L. Liang, Z. Li, and J. Q. Wang, "Improved detection of human respiration using data fusion based on a multistatic UWB radar," *Remote Sensing*, Vol. 8, No. 9, 773–791, 2016.
22. Lv, H., W. Li, Z. Li, Y. Zhang, T. Jiao, H. J. Xue, M. Liu, X. J. Jing, and J. Q. Wang, "Characterization and identification of IR-UWB respiratory-motion response of trapped victims," *IEEE Trans. Geosci. Remote Sens.*, Vol. 52, 7195–7204, 2014.
23. Yu, X., T. J. Jiao, H. Lv, Y. Zhang, Z. Li, and J. Q. Wang, "A new use of UWB radar to detecting victims and discriminating humans from animals," *2016 16th International Conference on Ground Penetrating Radar (GPR)*, 1–5, Hong Kong, China, June 2016.
24. Wang, Y., X. Yu, Y. Zhang, H. Lv, T. Jiao, G. Lu, W. Z. Li, Z. Li, X. Jing, and J. Wang, "Using wavelet entropy to distinguish between humans and dogs detected by UWB radar," *Progress In Electromagnetics Research*, Vol. 139, 335–352, 2013.
25. Yin, Y., X. Yu, H. Lv, F. G. Qi, Z. Q. Zhang, and J. Q. Wang, "Micro-vibration distinguishment of radar between humans and animals based on EEMD and energy ratio characteristics," *China Medical Devices*, Vol. 33, No. 10, 27–31, 2018.
26. Nunez, T. C., "Cotton BA transfusion therapy in hemorrhagic shock," *Curr. Opin. Crit. Care*, Vol. 15, 536–541, 2009.
27. Matsui, T., T. Ishizuka, B. Takase, M. Ishihara, and M. Kikuchi, "Non-contact determination of vital sign alterations in hypovolaemic states induced by massive haemorrhage: An experimental

- attempt to monitor the condition of injured persons behind barriers or under disaster rubble,” *Medical and Biological Engineering and Computing*, Vol. 42, No. 6, 807–811, 2004.
28. Wang, D. W., Y. Li, and R. Y. Peng, “Characters of the kinds and severity of injuries in deeply buried wounded personnel due to disaster and the monitoring of their vital sign,” *J. Trauma. Surg.*, Vol. 19, No. 10, 792–795, 2017.
 29. Azriel, P., R. Pizov, and C. Shamay, “Systolic blood pressure variation is a sensitive indicator of hypovolemia in ventilated dogs subjected to graded hemorrhage,” *Anesthesiology*, Vol. 67, 498–502, 1987.
 30. Stern, A., C. D. Susan, B. P. Steven, and X. Wang, “Effect of blood pressure on haemorrhage volume and survival in a nearfatal haemorrhage model incorporating a vascular injury,” *Annals of Emergency Medicine*, Vol. 22, 155–163, 1993.
 31. Fulop, A., Z. Turoczi, D. Garbaisz, L. Harsanyi, and A. Szijarto, “Experimental models of hemorrhagic shock: A review,” *European Surgical Research*, Vol. 50, No. 2, 57–70, 2013.
 32. Gutierrez, G. and H. D. Reines, “Wulf-gutierrez ME clinical review: Hemorrhagic shock,” *Crit. Care*, Vol. 8, 373–381, 2004.
 33. Shannon, C. E., “A mathematical theory of communication,” *ACM SIGMOBILE Mobile Computing and Communication Review*, Vol. 5, No. 1, 3–55, 1948.
 34. Hasan, A. A., S. P. Joseph, C. Z. Wendy, F. H. Daniel, and V. T. Nitish, “Wavelet entropy for subband segmentation of EEG during injury and recovery,” *Annals of Biomedical Engineering*, Vol. 31, 653–658, 2003.
 35. Cover, T. M. and P. E. Hart, “Nearest neighbor pattern classification,” *IEEE Transactions on Information Theory*, Vol. 13, No. 1, 21–27, 1967.
 36. Hand, D., H. Mannila, and P. Smyth, *Principles of Data Mining*, The MIT Press, 2013.
 37. Zhang, H., C. B. Alexander, M. Michael, and M. Jitendra, “SVM-KNN: Discriminative nearest neighbor classification for visual category recognition,” *2006 IEEE Computer Society Conference on Computer Vision and Pattern Recognition*, 2126–2136, New York, US, 2006.